

Effects of Fe doping in the colossal magnetoresistive $\text{La}_{1-x}\text{Ca}_x\text{MnO}_3$

K. H. Ahn, X. W. Wu, K. Liu, and C. L. Chien

Department of Physics and Astronomy, The Johns Hopkins University, Baltimore, Maryland 21218

The effect of Fe doping ($<20\%$) on the Mn site in the ferromagnetic ($x=0.37$) and the antiferromagnetic ($x=0.53$) phases of $\text{La}_{1-x}\text{Ca}_x\text{MnO}_3$ has been studied. Upon doping, no appreciable structure changes have been found in either series. However, conduction and ferromagnetism have been consistently suppressed by Fe doping. Colossal magnetoresistance has been shifted to lower temperatures, and in some cases enhanced by Fe doping. These results are not due to the strong lattice effects commonly seen in doping of the La sites. Rather, replacement of Mn^{3+} by Fe^{3+} depopulates the hopping electrons, and weakens the double exchange. The effect of Fe doping can be explained in terms of the band structure. © 1997 American Institute of Physics. [S0021-8979(97)73008-1]

During the last few years, perovskite manganites have attracted broad research interest, because of their unusual magnetic and transport properties, especially the colossal magnetoresistance (CMR)¹ phenomena. The prototype material $\text{La}_{1-x}\text{Ca}_x\text{MnO}_3$, with a rich phase diagram, has been studied extensively. Double exchange (DE)² has been featured prominently in the physics of the CMR materials. Doping the insulating LaMnO_3 material with the divalent ions (Ca, Ba, etc.) causes the conversion of a proportional number of Mn^{3+} to Mn^{4+} . The electrons hopping between the mixed Mn valence states then mediate ferromagnetism and conduction. The DE, and consequently, the physical properties of these materials, have been found to be particularly susceptible to lattice properties, such as the Mn–O–Mn bond angle and bond length.

To date, much of the exploration of the CMR materials has been done through doping the La sites with rare earths (Nd, Pr, etc.) of different sizes, which bring about strong lattice effects, and ultimately influencing the DE. However, fewer studies have been conducted on doping the Mn sites, which are at the heart of the DE. In this work, we have undertaken a study on the effects of doping the Mn sites by Fe in $\text{La}_{1-x}\text{Ca}_x\text{MnO}_3$, with $x=0.37$ and 0.53 . The starting materials of $\text{La}_{0.63}\text{Ca}_{0.37}\text{MnO}_3$ and $\text{La}_{0.47}\text{Ca}_{0.53}\text{MnO}_3$ are the FM and the AF phases, respectively, where CMR has been previously reported. Early studies have shown that in this Fe doping range, a direct replacement of Mn^{3+} by Fe^{3+} occurs.³ Also unique to this doping, Mn^{3+} and Fe^{3+} have identical ionic sizes.⁴ Consequently, the otherwise strong lattice effects can be bypassed, and the effects due to changes in the electronic structure become accessible.

Samples were fabricated with conventional solid state reaction methods. The chemical formula for the final compound is $\text{La}_{1-x}\text{Ca}_x\text{Mn}_{1-y}\text{Fe}_y\text{O}_3$, where $y < 0.20$ with $x=0.37$ and $x=0.53$. Powder x-ray diffraction shows single-phase tetragonally distorted perovskite structure for all the samples. For the series of $\text{La}_{0.63}\text{Ca}_{0.37}\text{Mn}_{1-y}\text{Fe}_y\text{O}_3$, no appreciable changes in the diffraction patterns induced by Fe doping has been observed. All the samples have the same lattice parameters of $a=b=5.45$ Å and $c=7.72$ Å. Similarly, the $\text{La}_{0.47}\text{Ca}_{0.53}\text{Mn}_{1-y}\text{Fe}_y\text{O}_3$ samples have the same lattice parameters of $a=b=5.42$ Å and $c=7.63$ Å. These results demonstrate the replacement of Mn by Fe without any structural change, and that the lattice effects have indeed

been bypassed. Our results are consistent with Jonker's earlier conclusion³ that Mn^{3+} is replaced by Fe^{3+} of the same size. As a further verification, we have employed standard ferrous sulfate and potassium permanganate titration method⁵ to determine the Mn valence. The titration results show ideal stoichiometry.

The temperature dependence of the magnetization M at $H=0.01$ T and the resistivity ρ at $H=0$ and at $H=5$ T for the $\text{La}_{0.63}\text{Ca}_{0.37}\text{Mn}_{1-y}\text{Fe}_y\text{O}_3$ series are shown in Figs. 1(a) and 1(b), respectively. The undoped sample undergoes a paramagnetic (PM) to FM transition, accompanied by a simultaneous insulator to metal transition, consistent with the results reported previously.⁶ As Fe is doped into the sample, both the FM transition temperature (T_c) and M are systematically lowered [Fig. 1(a)]. The sample resistivity ρ , on the other hand, increases with Fe doping, as shown in Fig. 1(b). In every case, a peak in ρ , characteristic of a metal–insulator transition, occurs near T_c . It is also noted that the large nega-

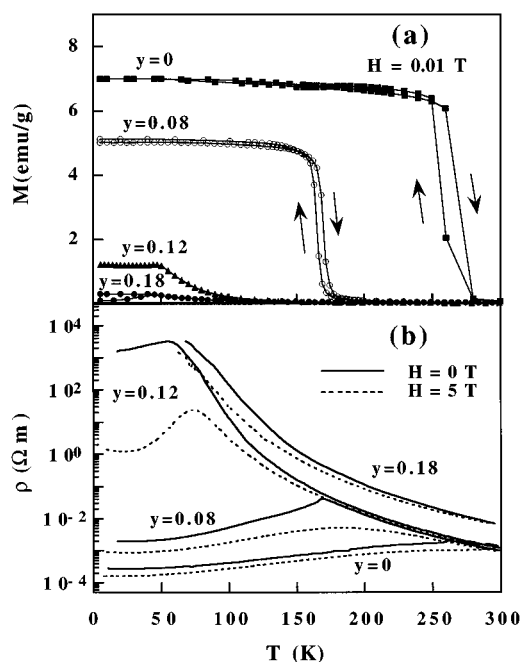


FIG. 1. Temperature dependence of (a) magnetization M in a 0.01 T field, and (b) resistivity ρ in zero (solid curves) and 5 T (dashed curves) magnetic field, for $\text{La}_{0.63}\text{Ca}_{0.37}\text{Mn}_{1-y}\text{Fe}_y\text{O}_3$ with $y=0, 0.08, 0.12$, and 0.18 .

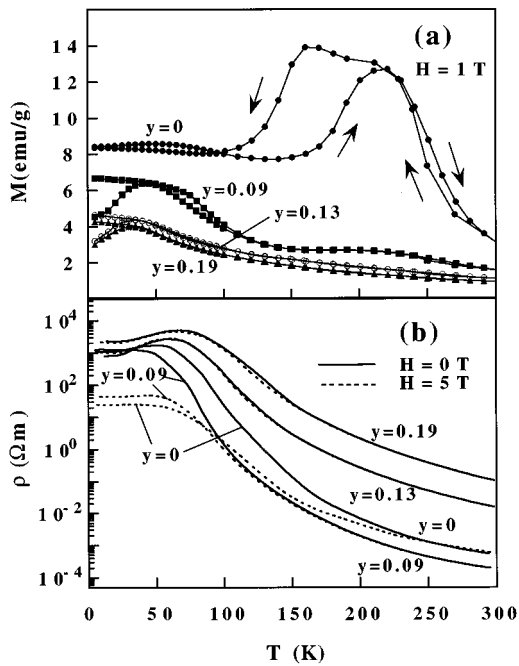


FIG. 2. Temperature dependence of (a) magnetization M in a 1 T field, and (b) resistivity ρ in zero (solid curves) and 5 T (dashed curves) magnetic field, for $\text{La}_{0.47}\text{Ca}_{0.53}\text{Mn}_{1-y}\text{Fe}_y\text{O}_3$ with $y=0, 0.09, 0.13$, and 0.19 .

tive magnetoresistance, or CMR, is dramatically enhanced, from 120% for the undoped sample ($y=0$) to three orders of magnitude for $y=0.12$. However, further doping to $y=0.18$, insulating behavior has been observed in the whole temperature range, with or without a 5 T field, although a sizable MR still remains.

The $\text{La}_{0.47}\text{Ca}_{0.53}\text{Mn}_{1-y}\text{Fe}_y\text{O}_3$ series, on the other hand, shows more complicated behavior. The magnetization data with $H=1$ T are shown in Fig. 2(a). The results for the undoped sample ($y=0$) are similar to those of $\text{La}_{0.5}\text{Ca}_{0.5}\text{MnO}_3$ previously reported,⁶ where an intermediate FM state was observed between the PM state at high temperatures and the AF state at low temperatures. Upon Fe doping to $y=0.09$, the intermediate FM state disappears and only the PM to AF transition remains. Further doping with Fe has a less effect on the PM to AF transition. It is noted that for the $y=0.09$ sample, an additional broad extremum in M at about 210 K is observed, possibly due to charge ordering.

The temperature dependence of the resistivity ρ at $H=0$ and at $H=5$ T of $\text{La}_{0.47}\text{Ca}_{0.53}\text{Mn}_{1-y}\text{Fe}_y\text{O}_3$ is shown in Fig. 2(b), which shows a qualitatively similar behavior among differently doped samples. With or without a magnetic field, the resistivity ρ increases with decreasing temperature, leveling off at 60 K. Fe doping generally increases the resistivity, although the initial Fe doping ($y=0.09$) actually lowers ρ . As for the magnetoresistance, the undoped ($y=0$) and the lightly doped ($y=0.09$) samples show negative MR by as much as two orders of magnitude at low temperatures. As the doping is further increased ($y=0.13$ and $y=0.19$), there is virtually no MR.

Magnetic hysteresis loops with field up to 5 T have been measured at 5 K for all samples. The magnetizations, nor-

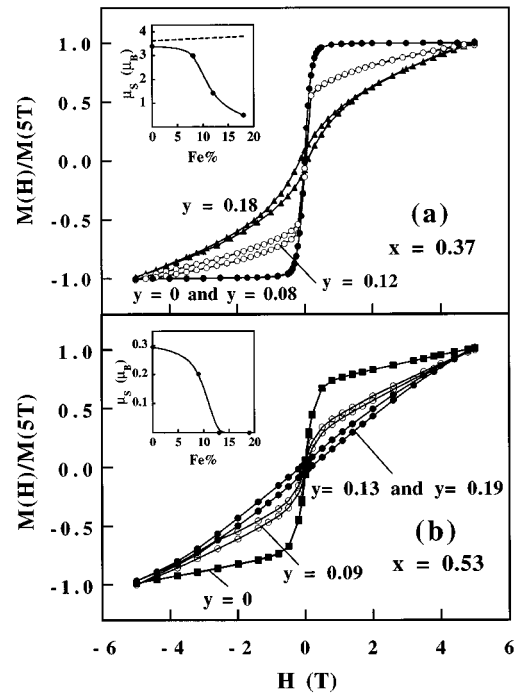


FIG. 3. Magnetic hysteresis loops measured at 5 K for $\text{La}_{1-x}\text{Ca}_x\text{Mn}_{1-y}\text{Fe}_y\text{O}_3$ with (a) $x=0.37$ and (b) $x=0.53$. The insets show the saturation magnetic moment μ_s per formula unit vs Fe content for each series. The dashed line indicates the values for full alignment of all the Mn and Fe moments.

malized to the value at 5 T, are shown in Fig. 3. For the $\text{La}_{0.63}\text{Ca}_{0.37}\text{Mn}_{1-y}\text{Fe}_y\text{O}_3$ series, shown in Fig. 3(a), samples with $y=0$ and $y=0.08$ show practically the same FM behavior. However, the magnetization curves for $y=0.12$ and $y=0.18$ are essentially a superposition of both the FM and AF components, indicating a canted spin state. The saturation magnetization of the FM component can be determined by extrapolating the linear part of the magnetization to $H=0$. These values, displayed as saturation moment per formula unit μ_s , are shown in the inset of Fig. 3(a). The dashed line in the inset represents the maximum value of μ_s , when all the Mn and Fe moments are aligned. The measured value of μ_s is nearly that of the fully aligned moment for the $y=0$ sample, but steadily declines upon Fe doping. Clearly, the presence of Fe, instead of enhancing, actually suppresses ferromagnetism.

The $\text{La}_{0.47}\text{Ca}_{0.53}\text{Mn}_{1-y}\text{Fe}_y\text{O}_3$ samples, as shown in Fig. 3(b), do not show pure FM behavior for any composition. Canted spin AF state has already set in for the samples with $y=0$ and $y=0.09$, both showing small FM components. The determined values of μ_s are only about $0.3 \mu_B$, about a factor of ten smaller than those shown in Fig. 3(a). Upon further Fe doping, no FM component but AF behavior can be observed.

It is well known that double exchange mediates ferromagnetism and metallic conduction. The transport and magnetic results shown above clearly demonstrate that the partial replacement of Mn by Fe favors insulating and AF behavior, opposing the effects of the double exchange. Since Fe doping is the direct replacement of Mn^{3+} by Fe^{3+} , the experi-

mental results suggest that the sites that are now occupied by Fe^{3+} can no longer effectively participate in the double exchange process. The mechanism that Fe^{3+} terminates the double exchange process arises purely from the electronic structure of the materials as we describe in the following.

In perovskite oxides, the $3d$ level of the Mn and Fe ions are known to split into $t_{2g}\uparrow$, $e_g\uparrow$, $t_{2g}\downarrow$, and $e_g\downarrow$ (in the order of increasing energy), due to the octahedral crystal field and the strong Hund's coupling. The electronic configurations are $t_{2g}\uparrow^3 e_g\uparrow^2$ for Fe^{3+} , $t_{2g}\uparrow^3 e_g\uparrow^1$ for Fe^{4+} and Mn^{3+} , and $t_{2g}\uparrow^3$ for Mn^{4+} , respectively. In a solid, these orbitals form bands. For these ions, the $t_{2g}\uparrow$ bands are fully occupied, the $t_{2g}\downarrow$ and $e_g\downarrow$ bands are empty, and the $e_g\uparrow$ bands, which can accommodate a maximum of two electrons per ion, play a crucial role. In a mixed system of Fe and Mn, the widths and energies of their $e_g\uparrow$ bands dictate the electron distribution of the Fe and Mn ions.

Early study on the conductivity of $\text{La}_{0.85}\text{Ba}_{0.15}\text{Mn}_{1-x}\text{Fe}_x\text{O}_3$ by Jonker³ has shown that for $0 < x < 0.85$, Fe^{3+} , Mn^{3+} , and Mn^{4+} are present, and for $0.85 < x < 1.00$, Fe^{3+} , Fe^{4+} , and Mn^{4+} are present. The existence of Fe^{3+} , Mn^{3+} , and Mn^{4+} in the range of $0 < x < 0.85$, indicates that the Fe $e_g\uparrow$ band is full and the Mn $e_g\uparrow$ band is less than half-filled. For $0.85 < x < 1.00$, the existence of Mn^{4+} , Fe^{3+} and Fe^{4+} means an empty Mn $e_g\uparrow$ band and a more than half-filled Fe $e_g\uparrow$ band. From this, it can be inferred that the bottom of the Mn $e_g\uparrow$ band should be at the same level as, or higher than, the top of the Fe $e_g\uparrow$ band. Thereby, the Fe $e_g\uparrow$ band remains completely filled as long as the Mn $e_g\uparrow$ band is partially filled.

Banks and Tashima have reached a similar conclusion by investigating the structural and conduction properties of a closely related system of $\text{La}_{1-x}\text{Ca}_x\text{Fe}_{1-x}\text{Mn}_x\text{O}_3$.⁷ They found that most Fe is present as Fe^{3+} and at least 97% of the Mn exists as Mn^{4+} . They proposed the presence of a small amount (less than 3%) of Mn^{3+} and Fe^{4+} to account for the conductivity behavior in their samples. This conclusion agrees with the above band structure, where the top of the Fe $e_g\uparrow$ band is nearly at the bottom of the Mn $e_g\uparrow$ band, except for a slight overlap (less than 3%) between the two, as shown in Fig. 4(a).

Our system of $\text{La}_{1-x}\text{Ca}_x\text{Mn}_{1-y}\text{Fe}_y\text{O}_3$ ($x=0.37$ and 0.53 , $y < 0.20$) is expected to have a similar band structure as that of $\text{La}_{1-x}\text{Ca}_x\text{Fe}_{1-x}\text{Mn}_x\text{O}_3$. The nominal stoichiometry is $\text{La}_{1-x}\text{Ca}_x^{2+}(\text{Mn}_x^{4+}\text{Mn}_{1-x-y}^{3+})\text{Fe}_y^{3+}\text{O}_3^{2-}$, for which both the Mn $t_{2g}\uparrow$ and Fe $t_{2g}\uparrow$ bands are filled. For the all important $e_g\uparrow$ bands, the Fe $e_g\uparrow$ band is completely filled, and $(1-x-y)/2(1-y)$ of the Mn $e_g\uparrow$ band is also filled. The latter filling factor is one half of the fraction of the Mn ions that are Mn^{3+} . The width of the Mn $e_g\uparrow$ band has been estimated to be about 1 eV.⁸ Assuming uniform filling for simplicity, and that the overlapped width of the Fe and Mn $e_g\uparrow$ bands is 3%, the Fermi surface would lie at $[(1-x-y)/2(1-y) - 0.03]$ eV above the top of the Fe $e_g\uparrow$ band. Using the composition values of x and y for our series, the Fermi surface will lie 0.14 to 0.29 eV above the top of the Fe $e_g\uparrow$ band, as shown in Fig. 4(b). This energy diagram clearly illustrates that electron hopping between Fe and Mn is impeded by the lack of available states in the Fe $e_g\uparrow$ band. The

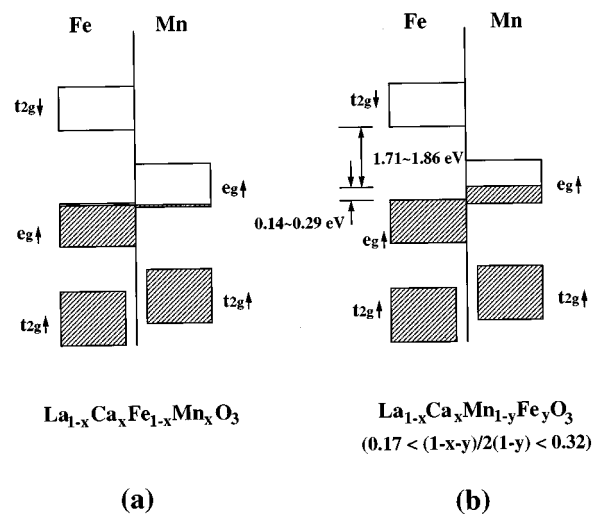


FIG. 4. Band structure of Fe and Mn in (a) $\text{La}_{1-x}\text{Ca}_x\text{Fe}_{1-x}\text{Mn}_x\text{O}_3$, where the bottom of the Mn $e_g\uparrow$ band lies slightly below the top of the Fe $e_g\uparrow$ band, and (b) $\text{La}_{1-x}\text{Ca}_x\text{Mn}_{1-y}\text{Fe}_y\text{O}_3$, where the Fe $e_g\uparrow$ band is completely filled and $(1-x-y)/2(1-y)$ of the Mn $e_g\uparrow$ band is filled.

only vacant states are in the Fe $t_{2g}\downarrow$ band, lying above the Fe $e_g\uparrow$ band, as shown in Fig. 4(b). However, Chainani *et al.*⁹ has shown that LaFeO_3 is an insulator with an intrinsic gap of about 2.0 eV, which implies that the Fe $t_{2g}\downarrow$ band is located about 2 eV above the top of the Fe $e_g\uparrow$ band, or 1.71~1.86 eV above the Fermi surface for our system, as shown in Fig. 4(b). It is clear that electron hopping from Mn to Fe is energetically forbidden even at room temperature. Consequently, only the Mn $e_g\uparrow$ band is electronically active, where electron hopping can occur between Mn^{3+} and Mn^{4+} . Since Fe^{3+} replaces Mn^{3+} , doping with Fe causes a depletion of the $\text{Mn}^{3+}/\text{Mn}^{4+}$ ratio, the population of the hopping electrons, and the number of available hopping sites. Thus, double exchange is suppressed, resulting in the reduction of ferromagnetism and metallic conduction.

In summary, we have observed suppression of ferromagnetism and conduction in both the FM and the AF phases of $\text{La}_{1-x}\text{Ca}_x\text{MnO}_3$ by doping Fe on the Mn sites. The usually dominant lattice effects have been bypassed due to the identical size of Mn^{3+} and Fe^{3+} . These results originate from the reduction of double exchange due to the depopulation of hopping electrons by the Fe doping.

This work is supported by NSF Grant No. DMR 95-01195.

¹R. von Helmolt, J. Wecker, B. Holzapfel, L. Schultz, and K. Samwer, Phys. Rev. Lett. **71**, 2331 (1993); S. Jin, T. H. Tiefel, M. McCormack, R. A. Fastnacht, R. Ramesh, and L. H. Chen, Science **264**, 413 (1994).

²C. Zener, Phys. Rev. **82**, 403 (1951); P.-G. de Gennes, *ibid.* **118**, 141 (1960).

³G. H. Jonker, Physica (Amsterdam) **20**, 1118 (1954).

⁴R. D. Shannon, Acta Crystallogr. Sec. A **32**, 751 (1976).

⁵H. L. Yakel, Jr., Acta Crystallogr. **8**, 394 (1955).

⁶P. Schiffer, A. P. Ramirez, W. Bao, and S.-W. Cheong, Phys. Rev. Lett. **75**, 3336 (1995).

⁷E. Banks and N. Tashima, J. Appl. Phys. **41**, 1186 (1970).

⁸J. M. D. Coey, M. Viret, L. Ranno, and K. Ounadjela, Phys. Rev. Lett. **75**, 3910 (1995).

⁹A. Chainani, M. Mathew, and D. D. Sarma, Phys. Rev. B **48**, 14818 (1993).